An experimental study of optical anisotropy of blue-phase liquid crystals as a function of alignment layers

Sumanyu Chauhan[a,b], Markus Wahle[a], Grigory Lazarev[a], Dieter Cuypers[b], and Herbert De Smet[b]

[a]Huawei Munich Research Center, 80992 Munich, Germany
[b]Centre for Microsystems Technology (CMST), imec and Ghent University, 9000 Gent, Belgium

ABSTRACT

The growing requirements for ultrafast communication speeds are constantly pushing the need to explore new devices and materials to reduce bottlenecks in optical communication networks. One such device is a phase-only spatial light modulator implemented using liquid crystal on silicon. Achieving this requires polarization-independent and fast-switching optical materials. Blue-phase liquid crystal is one such candidate. Popular opinion is that blue-phase liquid crystal is polarization-independent. In this study using microscopic and polarimetric methods, we demonstrate that in the off-state of blue-phase, the alignment layers affect the optical polarization behavior.

Keywords: blue phase liquid crystals, alignment layers, polarization optics

1. INTRODUCTION

The most basic form of liquid crystals (LCs) are nematics (N or NLCs). However, due to spontaneous or induced chirality nematics can take the form of cholesteric liquid crystals (ChLC) or chiral nematics (N*) as shown in fig. 1.[1] When chirality increases further in the ChLCs, it causes frustration in the elastic structure which results in the ChLC to spontaneously self-assemble into cubic lattices or amorphous network of disclination lines to balance the energy and entropy of the system.[2] These self-assembled nano-structures form a thermodynamically distinct phase are called blue-phase (BP) liquid crystals.

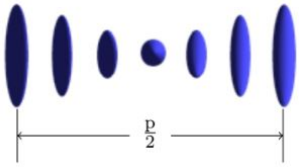

Figure 1: Helical structure of the chiral nematic phase. A 180° rotation of the director is shown, which is equal to half the cholesteric pitch (p). Adapted from ref.[3]

BPs exhibit a complex, regular three-dimensional structure with lattice dimensions in the visible or UV range. The cubic lattices formed with double-twist cylinders (DTCs) are as shown in fig. 2. These are known as BP-I, and BP-II.[4] Apart from BP-I and BP-II, a third BP modification is known, blue-phase III (BP-III). It has no cubic symmetry, instead, the DTCs are randomly distributed without long-range order.[5]

The diameter δ of a double-twist cylinder corresponds to one-quarter pitch. When DTCs are packed in a cubic lattice, defects occur in the space between three neighboring DTCs, where the director does not change continuously. In the core of these so-called disclination lines all orientational order is lost. In fig. 2, cubic

Fore more information contact:
Sumanyu Chauhan: E-mail: sumanyu.chauhan@huawei.com, Telephone: +49 172 7237 217
Markus Wahle: E-mail: markus.wahle@huawei.com, Telephone: +33 (0)1 98 76 54 32

unit cells and disclination lines are shown for the body-centered cubic (bcc) (figs. 2b and 2c) and simple cubic (sc) (figs. 2d and 2e) structures called blue-phase I (BP-I) and blue-phase II (BP-II), respectively. The lattice constant a of the unit cell is related to the pitch as follows: in BP-I the relation is given by $a = 4\delta \approx p$ and in blue-phase II (BP-II) it is $a = 2\delta \approx p/2$ (compare figs. 2b and 2d, respectively). Because of the defect structure, BPs typically exist in a small temperature range (< 1 K) between the chiral nematic and the isotropic phase (Iso).

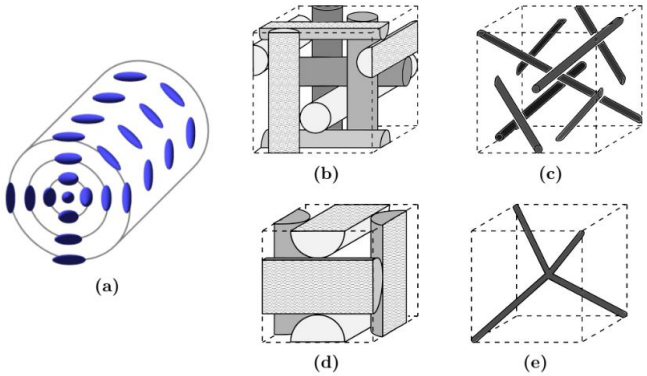

Figure 2: Blue-phase structure: The double-twist cylinder (a) as a basic structure is arranged in unit cells with different symmetries, body-centered cubic for BP-I (b) and simple cubic for BP-II (d). Discontinuities in the change of molecular orientations occur in the space between three double-twist cylinders. These disclinations are shown for BP-I (c) and BP-II (d), respectively. Adapted from ref.[3]

In blue-phases Bragg scattering can be observed. BPs may show several selective reflections. The Bragg wavelength is:

$$\lambda_{\text{Bragg}} = \frac{2a.\bar{n}_{\text{BP}}.\sin\theta}{(h^2+k^2+l^2)^{1/2}} \tag{1}$$

with the averaged refractive index

$$\bar{n}_{\text{BP}} = \sqrt{\frac{1}{3}n_e^2 + \frac{2}{3}n_o^2} \tag{2}$$

where n_e is the extraordinary refractive index and n_o is the ordinary refractive index of the constituent NLC.

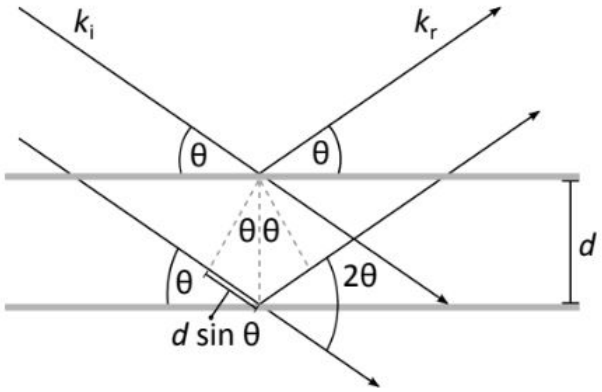

Figure 3: Incident light with parallel wave vectors k_i is reflected k_r at different lattice planes. For phase retardations equal to $2d\sin\theta$ the reflected wavelengths interfere constructively and Bragg reflections are observed. Adapted from ref.[3]

The reflected wavelengths depend on the orientation of the lattice planes with respect to the incident beam as shown in the schematic in fig. 3, where (h, k, l) are the Miller indices of a set of planes. Possible combinations of

the Miller indices depend on the BP symmetry. In simple cubic symmetry all h, k, l are allowed, while in body-centered cubic systems, the sum $h + k + l$ needs to be even.[6] Based on the selection rules for Bragg reflections in blue-phases[7] the lattice planes can be assigned to the different reflection wavelengths. The ratio of adjacent reflection wavelengths is $1/\sqrt{2}, 1/\sqrt{3}, 1/\sqrt{4}, \ldots$ in BP-I and BP-II.[8] For normal light incidence ($\theta = \pi/2$), Bragg reflections observed for BPs are circularly polarized.[9]

Blue-phases are optically isotropic and show no birefringence. However, they are locally anisotropic in volumes that are small compared to the unit cell. Due to this structural complexity, BPs exhibit 3D photonic bandgap,[10] low or no dependence on the state of incident polarization,[11] and sub-millisecond response.[12] Certain applications in micro-lens arrays[13–15] and phase-only LCoS[16–20] demand that the ellipticity of the linearly polarized incident light does not change. This makes it imperative to study the polarization properties of blue-phase to validate its suitability for such applications. In this paper, we further explore the off-state (i.e. no external electric field) interaction of blue-phase with plane-polarized light, compare results with a single known previous study of this nature[11] and present the scope of further research in this area.

2. METHODS

Materials

To obtain the blue phase, a nematic mixture HTG135400-100 from Jiangsu Hecheng Display Technology Co., Ltd (HCCH) is doped with 3.04 wt.% of S5011, a chiral dopant (CD, 99.9% purity) from HCCH with high a helical twisting power of 115 μm^{-1}. Using a high-HTP CD improves the long-term stability of the mixture because the low amount prevents crystallization.[21] The material property parameters of the nematic host are summarized in table 1.

Table 1: Materials parameters of the nematic mixture.

LC parameter	**Value**
K_{11}	5.02 (pN)
K_{22}	2.51 (pN)
K_{33}	10.96 (pN)
γ_1	2.761 (PaS)
n_e	1.67
n_o	1.505
Δn	0.165
$e_{\parallel}$	47.6
$e_{\perp}$	11.5
Δe	36.1
Phase temperatures	Cr. 0°C N 80°C Iso.

Test cells

The liquid crystal test cells used in this study were purchased from EHC, Japan. Three vertical field switching (VFS) mode cells were used in this study. Each of the cells exhibits a different alignment, namely homeotropic, homogeneous, and no alignment conditions respectively. A description of the parameters of the test cell used in the study is provided in table 2.

Characterization of BPLC

The BPLC mixture was vortex mixed, the mixture was heated beyond the isotropic phase temperate, and capillary filled in the cells while still in the isotropic phase. The BPLC inside the cell geometries was characterized by microscopic methods to obtain the phase temperature range of the BPs. The heat stage with the test cell containing the BPLC sample was placed between crossed polarizers and the microscope was operated in reflection mode. A camera - Alvium 1800 U-508c by Allied Vision was attached to the microscope. It was used to capture the microscopic images of the BPs. The camera was manually color corrected for the white balance. A

Table 2: Parameters of the VFS test cells used.

Cell parameter	**Value / type**
Pixel size	10 mm X 10 mm
Glass thickness	0.7 mm
Glass material	Borosilicate
ITO thickness	200-400 Å
ITO resistivity	100 Ω
Seal material	Epoxy resin
Cell gap	10 μm
Alignment materials	
Polyimide	LX - 1400 by Hitachi
Surface-active agent	$([(C_{16}H_{33})N(CH_3)_3]Br$

polarized optical microscope (POM) from Leica – D27000M was used to study the phase transition textures and temperatures. The reflected light which is circularly polarized passes partly through the second linear polarizer (analyzer).

Optical benchtop setup

An optical benchtop was set up to study the polarization properties of BPs. The schematic for the optical setup used for the experiment is shown in figure 4. It consists of:

- a laser (TGSL-640-15-RSP-G-SWC from Osela, Canada) with center wavelength 635 nm,
- an iris (I),
- two broadband linear polarizers (LP1 and LP2) to control the optical power,
- a half-waveplate (HWP) to rotate the plane of the polarized light incident on the sample,
- a high precision heat stage (LTS120 Peltier system and T96 Peltier controller from Linkam, UK) with an aperture to allow for the transmission of the laser beam through the heat stage and the cell,
- a polarimeter (PAX1000VIS from Thorlabs, Germany).

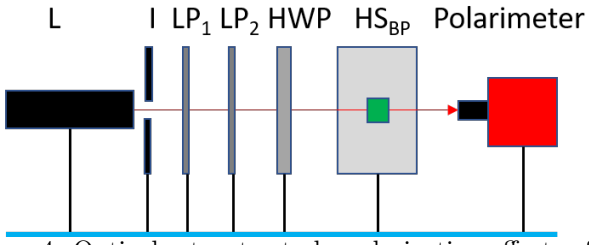

Figure 4: Optical setup to study polarization effects of BPs.

3. RESULTS

First, the phase temperature range of BPs in various cells was determined. These are presented in table 1. The phase textures were captured in an image lapse. The textures of BP at 71.4°C in cells with homogeneous alignment, no alignment, and homeotropic alignment are shown in the figure. Each of these cells was mounted on the heat stage, heated to isotropic and cooled to 71.4° at the rate of 1° / min. Later on, the plane of linear polarized light incident on the sample was rotated with the help of HWP and DoP and ellipticity of the transmitted light was measured in transmission through the polarimeter, shown in table 4.

Table 3: Temperature range of BP1 in test cells with different alignment conditions.

Alignment layer	**BP temperature range**
Homogenous	70.9-74.3 ° C
None	70.6-74.4 ° C
Homeotropic	70.9-74.5 ° C

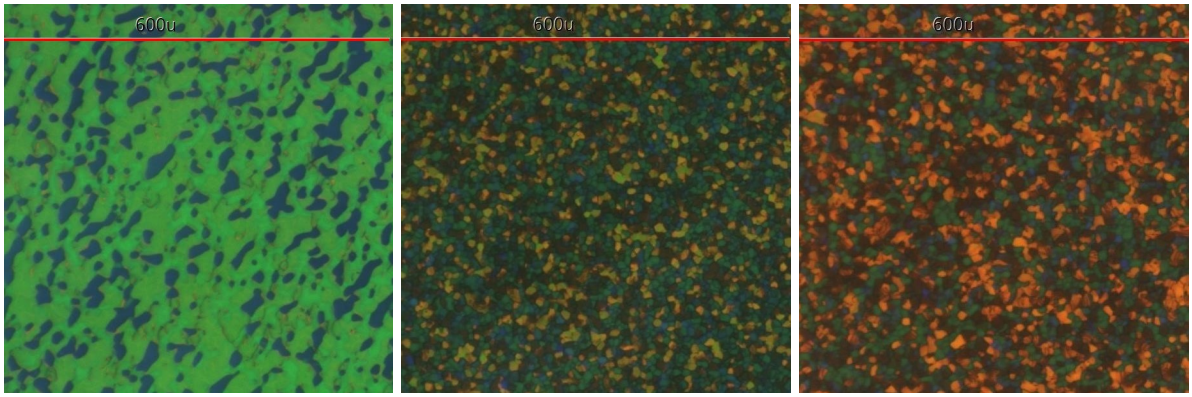

(a) BP in test cell with homogeneous alignment.

(b) BP in test cell with no alignment layer.

(c) BP in test cell with homeotropic alignment.

Figure 5: POM images of BPs in reflection mode. BPs were confined in test cells with various alignment conditions. Images were captured when the test cells were at 71.4°C. Scale bars (red) are 600 um.

Table 4: Modulation of light polarization in the off state of BPs in different alignment layers.

Sample	**Ellipticity**		**DoP**	
	Min	Max	Min	Max
No cell	0 °	1.3 °	95.07 %	99.85 %
Homogeneous	0 °	1.5 °	95.42 %	99.81 %
No anchoring	0 °	5.24 °	93.74 %	98.05 %
Homeotropic	0 °	10.16 °	87.02 %	92.65 %

4. DISCUSSION

The degree of polarization (DoP) is used to describe the portion of an electromagnetic wave that is polarized. DoP is calculated as the fraction of the total power that is carried by the polarized component of the wave. Therefore, a perfectly polarized wave is desired to improve the efficiency of the system. Ellipticity or ellipticity angle is an indication of the deviation from the state of linear polarized light. For linear polarized light ellipticity angle = 0 °.

Certain applications demand that the ellipticity of the linearly polarized incident light does not change[13–15] which makes it imperative to study the polarization properties of blue-phase to validate its suitability for such applications. To the best knowledge of the authors, the only other experimental study of polarization effects in blue-phase is ref.[11] However, this does not include DoP measurements which are an important metric for high-efficiency optical systems. In this study, we use different alignment chemicals as mentioned in table 2 for the homeotropic and homogeneous conditions.

Different alignment conditions provide different anchoring strengths and anchoring energies to the BP. Thus, different alignment conditions induce a preferred lattice orientation. Polarized optical microscopy (POM) in reflection mode of BPs in test cells with different alignment conditions in fig. 5 shows many colorful platelets. Each colorful platelet represents a domain of BP lattices with the same orientation of the lattice planes. Each unique lattice plane reflects a distinct Bragg wavelength as described by eq. 1.

For example, in the case of the homogeneous alignment (fig.5a), domains consisting of lattice orientations reflecting green and blue light are dominant. For the test cell with no-alignment layer (fig. 5b), lattices with random orientation satisfying eq. 1 are seeded on the surface of the test cell. Similarly, for the cell with

homeotropic alignment conditions (fig. 5c), lattices with random orientation satisfying eq. (1) are seeded on the surface of the test cell.

Each of these cells was separately mounted on the heat stage, in an optical assembly shown in fig. 4. The test cell was heated to an isotropic temperature and cooled to 71.4 °C then held at that temperature. An iris was used to reduce the spot size of the laser with a wavelength of 633. Two linear polarizers were used to clean up any stray polarization. The resulting linear polarized light was rotated with the help of a half-waveplate. The linear polarized laser light incident on the BP test cells is transmitted through the aperture on the heat stage and the polarization state was measured with the polarimeter. The center of the beam spot was well aligned with the center of the hot stage aperture and the center of the polarimeter sensor.

As the slow-axis of the HWP was rotated by an angle θ wrt. polarization direction of the incoming light, the plane of the linear polarized light incident on the sample was thus rotated by 2θ wrt. the initial position of the slow-axis of the HWP. It was noted that the DoP values changed significantly in all cases. Maximum and minimum values of DoP in the case of each test cell were noted as shown in table 4, including the control (no cell). The maximum and minimum values of ellipticity angles were also noted for each case in table 4. It has to be emphasized that the maximum and minimum values of DoP and ellipticity angles are independent of each other.

BP test cell with homogeneous alignment predominantly reflects green and blue light (fig. 5a), these Bragg reflection wavelengths are far away from the wavelength of the incident laser (635 nm), therefore incident light gets transmitted through it. For the test cell with no-alignment layer the predominant Bragg reflections (fig. 5b) are green and yellow, the wavelengths of these reflection bandgaps are closer to the wavelength of the incident laser light, so some interaction can be assumed. Finally, in the case of the homeotropic alignment layer, the orientation of lattices is such that the Bragg reflections or the color of the platelets (fig. 5b) are much closer to the wavelength of the incident laser. The closeness of the Bragg reflection to the wavelength of the incident laser light points to the change in the polarization state as noted in table 4. The maximum change in ellipticity happened in the case of the homeotropic alignment condition where Bragg reflections are closest to the wavelength of the incident laser (635 nm). The minimum change in the ellipticity happened in the case of homogeneous alignment conditions where Bragg reflections are much farther away from the wavelength of the incident laser (635 nm).

By using new types of alignment layers materials, claims of change in the ellipticity of linear polarized light in[11] have been corroborated. However, to fully understand the mechanism of alignment layer-induced change in the polarization properties further study is needed.

5. FUTURE WORK

This study has been limited to BP-I in the off-state at 71.4 °C, using laser light with a wavelength of 635 nm. To ascertain the BP state, spectroscopic measurements should be added. To confirm the band-edge effect on the polarization properties, a blue, and green laser can be used. Furthermore, wavelengths beyond the visible region, into the infrared region could be used to test the band-edge hypothesis of the polarization properties of BP. Currently, it remains unclear why DoP changes in the control condition. It could be due to the imperfections of the polarizers but this still needs to be ascertained. To expand the scope of this study, measurements can be made for the on-state of BP-II as well as for different alignment chemicals and methods.

REFERENCES

[1] Bahr, C. and Kitzerow, H.-S., [*Chirality in liquid crystals*], Springer (2001).

[2] Selinger, J. V., [*Introduction to the theory of soft matter: from ideal gases to liquid crystals*], Springer (2016).

[3] Nordendorf, G., *Effects of monomer composition on the electro-optic performance of polymer-stabilized blue phase liquid crystals*, PhD thesis, Paderborn University (2015).

[4] Meiboom, S., Sethna, J. P., Anderson, P., and Brinkman, W., "Theory of the blue phase of cholesteric liquid crystals," *Physical Review Letters* **46**(18), 1216 (1981).

[5] Stegemeyer, H., Blümel, T., Hiltrop, K., Onusseit, H., and Porsch, F., "Thermodynamic, structural and morphological studies on liquid-crystalline blue phases," *Liquid Crystals* **1**(1), 3–28 (1986).

[6] Johnson, D., Flack, J., and Crooker, P., "Structure and properties of the cholesteric blue phases," *Physical Review Letters* **45**(8), 641–644 (1980).

[7] Hornreich, R. and Shtrikman, S., "Optical selection rules and structures of cholesteric blue phases," *Physics Letters A* **82**(7), 345–349 (1981).

[8] Bahr, C. and Kitzerow, H.-S., [*Chirality in liquid crystals*], Springer-Verlag, New York (2001).

[9] Flack, J. and Crooker, P., "Polarization and pitch dependence of cholesteric blue-phase structures," *Physics Letters A* **82**(5), 247–250 (1981).

[10] Chen, C.-W., Hou, C.-T., Li, C.-C., Jau, H.-C., Wang, C.-T., Hong, C.-L., Guo, D.-Y., Wang, C.-Y., Chiang, S.-P., Bunning, T. J., et al., "Large three-dimensional photonic crystals based on monocrystalline liquid crystal blue phases," *Nature communications* **8**(1), 1–8 (2017).

[11] Orzechowski, K., Sierakowski, M. W., Sala-Tefelska, M., Joshi, P., Woliński, T. R., and De Smet, H., "Polarization properties of cubic blue phases of a cholesteric liquid crystal," *Optical Materials* **69**, 259–264 (2017).

[12] He, S., Lee, J.-H., Cheng, H.-C., Yan, J., and Wu, S.-T., "Fast-response blue-phase liquid crystal for color-sequential projection displays," *Journal of Display Technology* **8**(6), 352–356 (2012).

[13] Tian, L.-L., Zhou, Y., Li, L., and Chu, F., "Two-dimensional blue phase liquid crystal microlens array with low driving voltage and polarization independence," *Liquid Crystals* **49**(6), 836–844 (2022).

[14] Lin, Y.-H. and Chen, H.-S., "Electrically tunable-focusing and polarizer-free liquid crystal lenses for ophthalmic applications," *Opt. Express* **21**, 9428–9436 (Apr 2013).

[15] Chu, F., Guo, Y.-Q., Zhang, Y.-X., Duan, W., Zhang, H.-L., Tian, L.-L., Li, L., and Wang, Q.-H., "Four-mode 2d/3d switchable display with a 1d/2d convertible liquid crystal lens array," *Opt. Express* **29**, 37464–37475 (Nov 2021).

[16] Hyman, R. M., Lorenz, A., Morris, S. M., and Wilkinson, T. D., "Polarization-independent phase modulation using a blue-phase liquid crystal over silicon device," *Applied optics* **53**(29), 6925–6929 (2014).

[17] Sun, C. and Lu, J., "A polarization-independent blue phase liquid crystal on silicon with low operation voltage," *Scientific Reports* **9**(1), 1–6 (2019).

[18] Peng, F., Lee, Y.-H., Luo, Z., and Wu, S.-T., "Low voltage blue phase liquid crystal for spatial light modulators," *Optics letters* **40**(21), 5097–5100 (2015).

[19] Frisken, S. J., Baxter, G. W., and Wu, Q., "Polarization-independent lcos device," (June 23 2015). US Patent 9,065,707.

[20] Chu, D., Collings, N., Moore, J. R., Pivnenko, M., and Robertson, B., "Optical device and methods," (Sept. 26 2017). US Patent 9,774,930.

[21] Joshi, P., De Smet, J., Shang, X., Willekens, O., Cuypers, D., Van Steenberge, G., Chojnowska, O., Kula, P., Van Vlierberghe, S., Dubruel, P., et al., "Long term stability of polymer stabilized blue phase liquid crystals," *Journal of Display Technology* **11**(9), 703–708 (2015).